SUPPLEMENTARY MATERIAL

Figures S1-S12.

Movies 1-5.

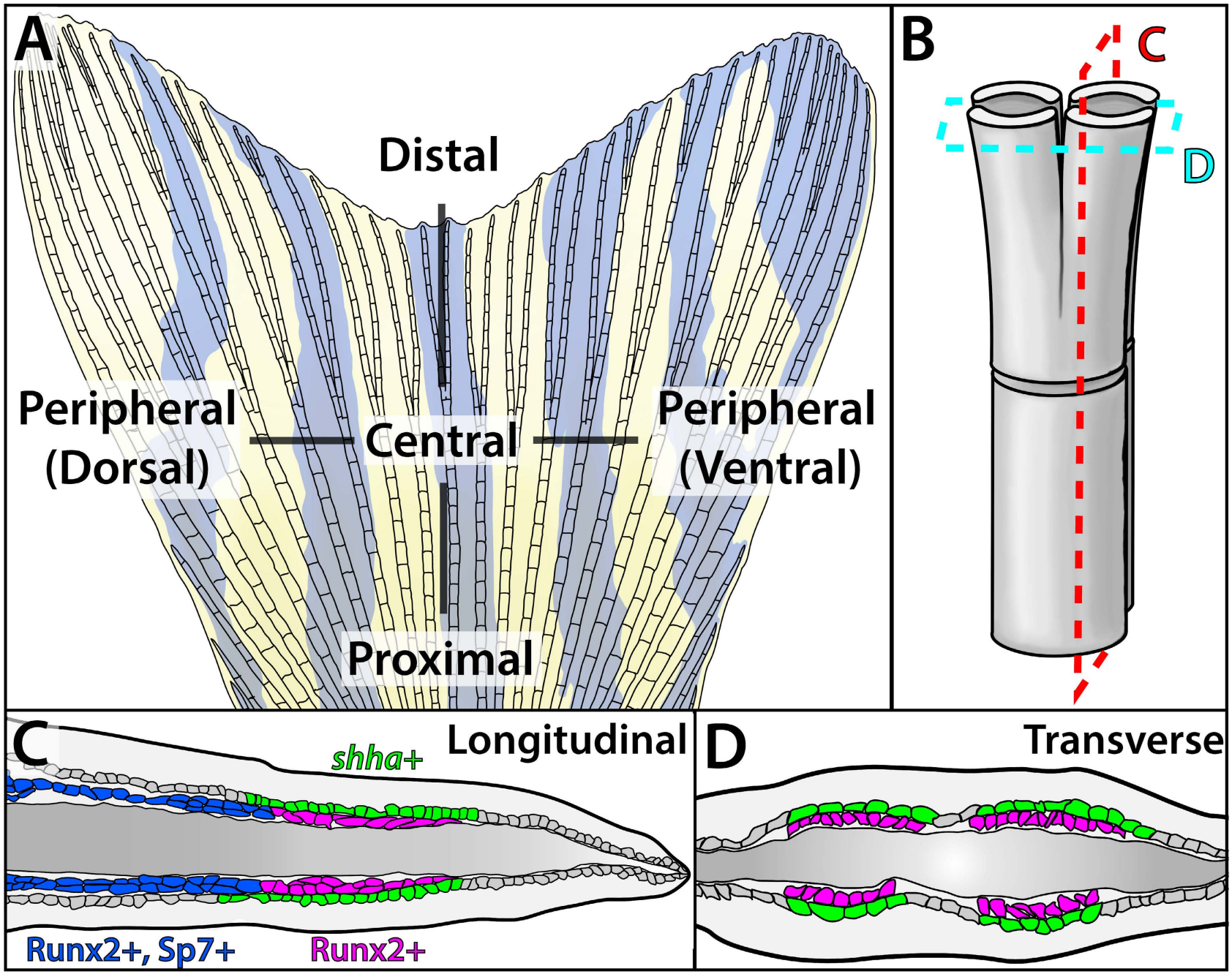

Supplemental Figure 1

Figure S1. Schematic of caudal fin skeletal anatomy.

(A) Schematic of an adult zebrafish caudal fin. The caudal fin skeleton comprises 18 bony rays (lepidotrichia), of which the inner 16 branch at least once. (B) Cartoon rendering of a skeletal ray branch point. Two opposed hemi-cylindrical calcified hemi-rays form each ray. Branching produces two equally sized daughter rays. (C, D) Colored tracings of longitudinal (C) and transverse (D) sections through a branching lepidotrichia. Distal domains of *shha*-expressing basal epidermal cells (basal epidermis, green) directly neighbor Runx2+ pre-osteoblasts (magenta). Those basal epidermal cells distally beyond pre-osteoblast pools lose *shha* expression. *shha*+ basal epidermis and pre-osteoblast domains both split peripherally as branching initiates. As the fin extends, the distal Runx2+ pre-osteoblast pool generates differentiating Runx2/Sp7+ osteoblasts (purple) that eventually mature into proximal sp7+ bone-forming cells (blue).

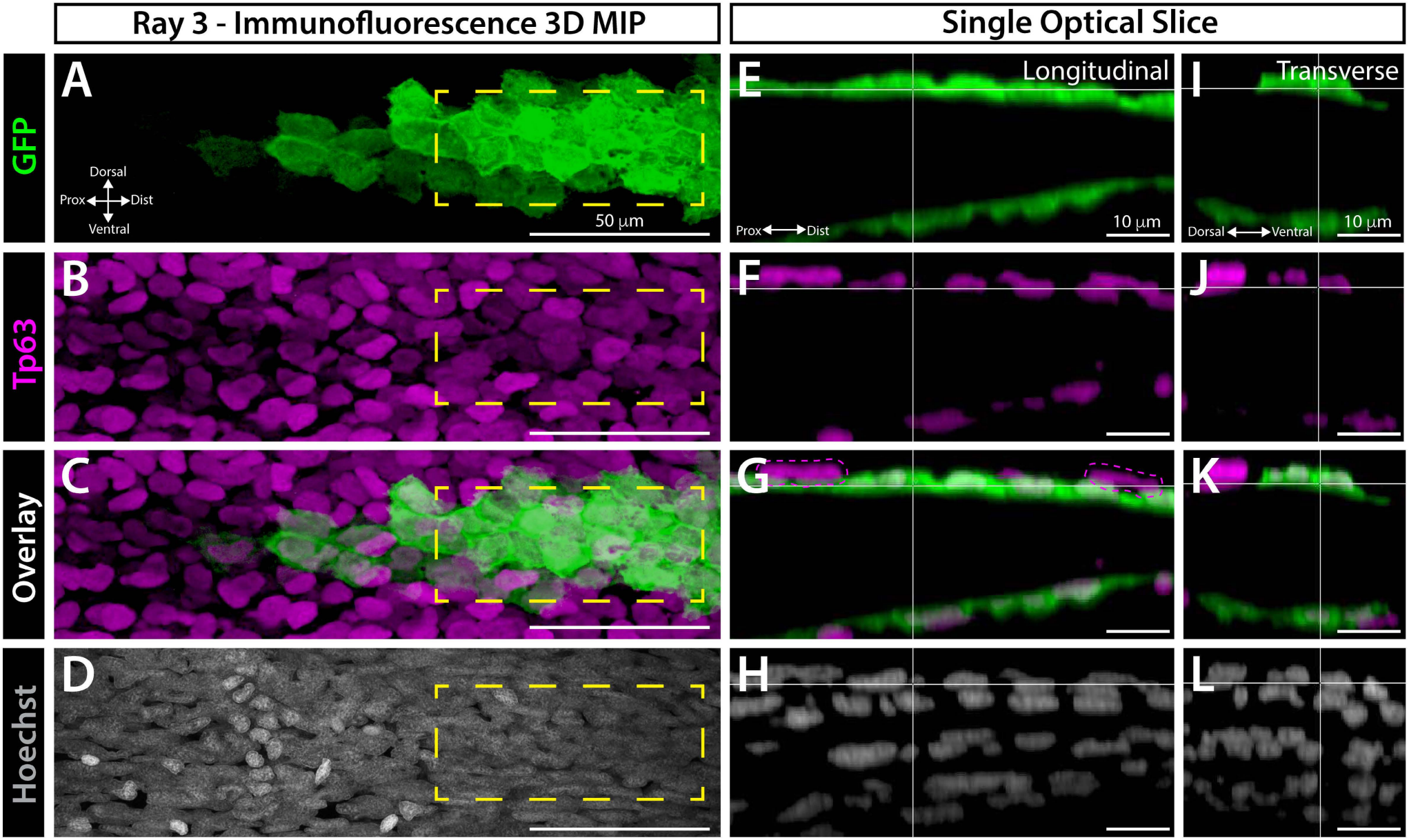

Supplemental Figure 2

Figure S2. *shha* is expressed in a single layer of distal basal epidermal cells in developing caudal fins.

3D reconstructed sectional views of dorsal ray 3 from a whole mount immunostained 23 dpf *shha:GFP* caudal fin. Panels show GFP (green, A, E, I), the basal epidermal marker Tp63 (magenta, B, F, J), GFP and Tp63 overlays (C, G, K; G and K are reproduced in Figure 1), and Hoechst-stained nuclei (white, D, H, I). (A-D) Maximum intensity projection (MIP) of the "native" frontal view. (E-L) Reconstructed single optical slice equivalents showing longitudinal (E-H) and transverse (I-L) planar views of the dashed yellow boxed regions in (A-D). Shha-expressing cells (as marked by GFP) define the innermost basal epidermal cell layer and all co-express Tp63. An occasional single-positive Tp63+ basal epidermis (representative cell in magenta dashed lines, G) is found in the suprabasal layer. Scale bars and orientations are indicated.

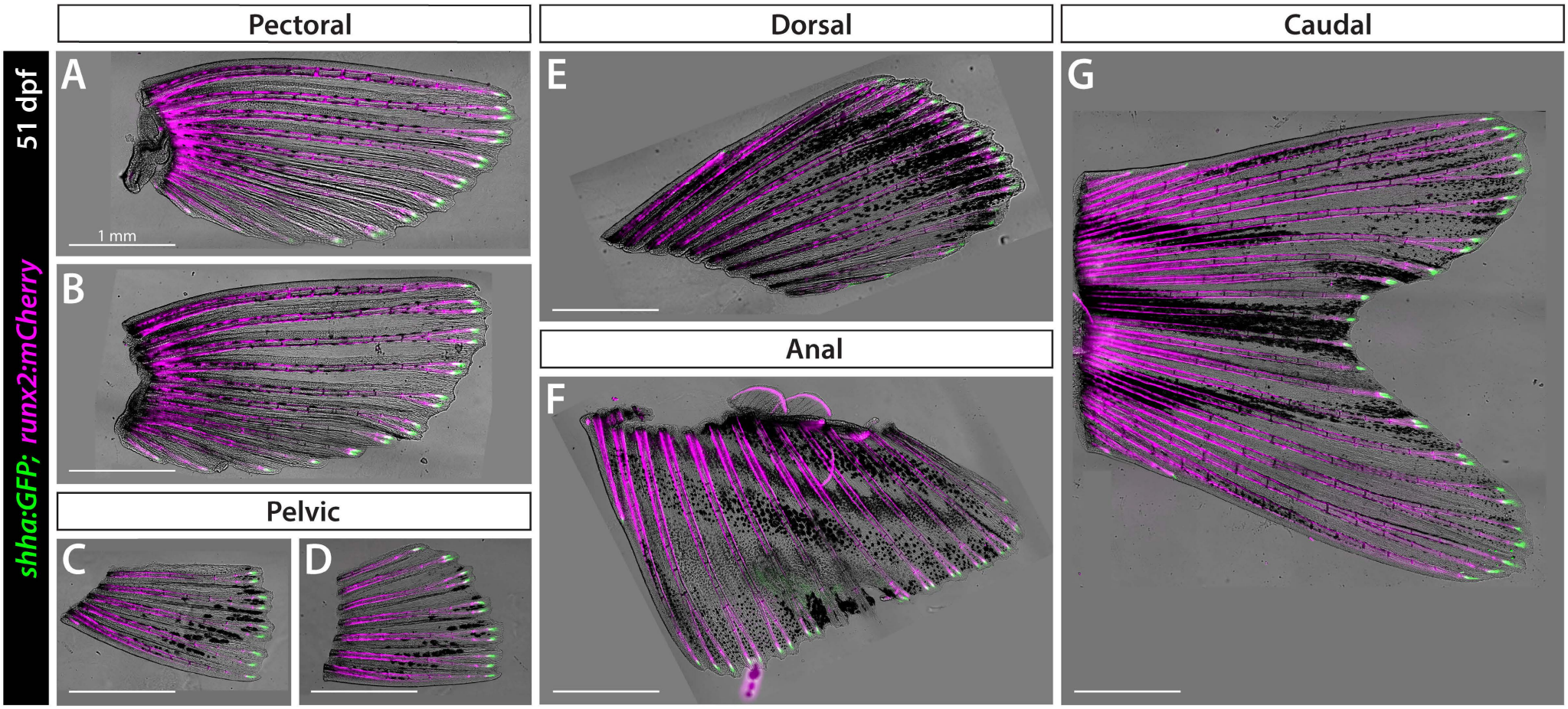

Supplemental Figure 3

Figure S3. Distal *shha* expression is conserved across developing fins.

Dissected fins from a representative 51 dpf *shha:GFP;runx2:mCherry* fish. Zebrafish have 7 fin appendages: the paired pectoral (A, B) and pelvic (C, D) fins and unpaired dorsal (E), anal (F), and caudal (F) fins. All have branched rays marked by *runx2:mCherry* (magenta) with *shha:GFP+* domains (green) at the distal end of each developing ray. All images are brightfield/GFP/mCherry overlays and sized to the same scale (1 mm scale bars).

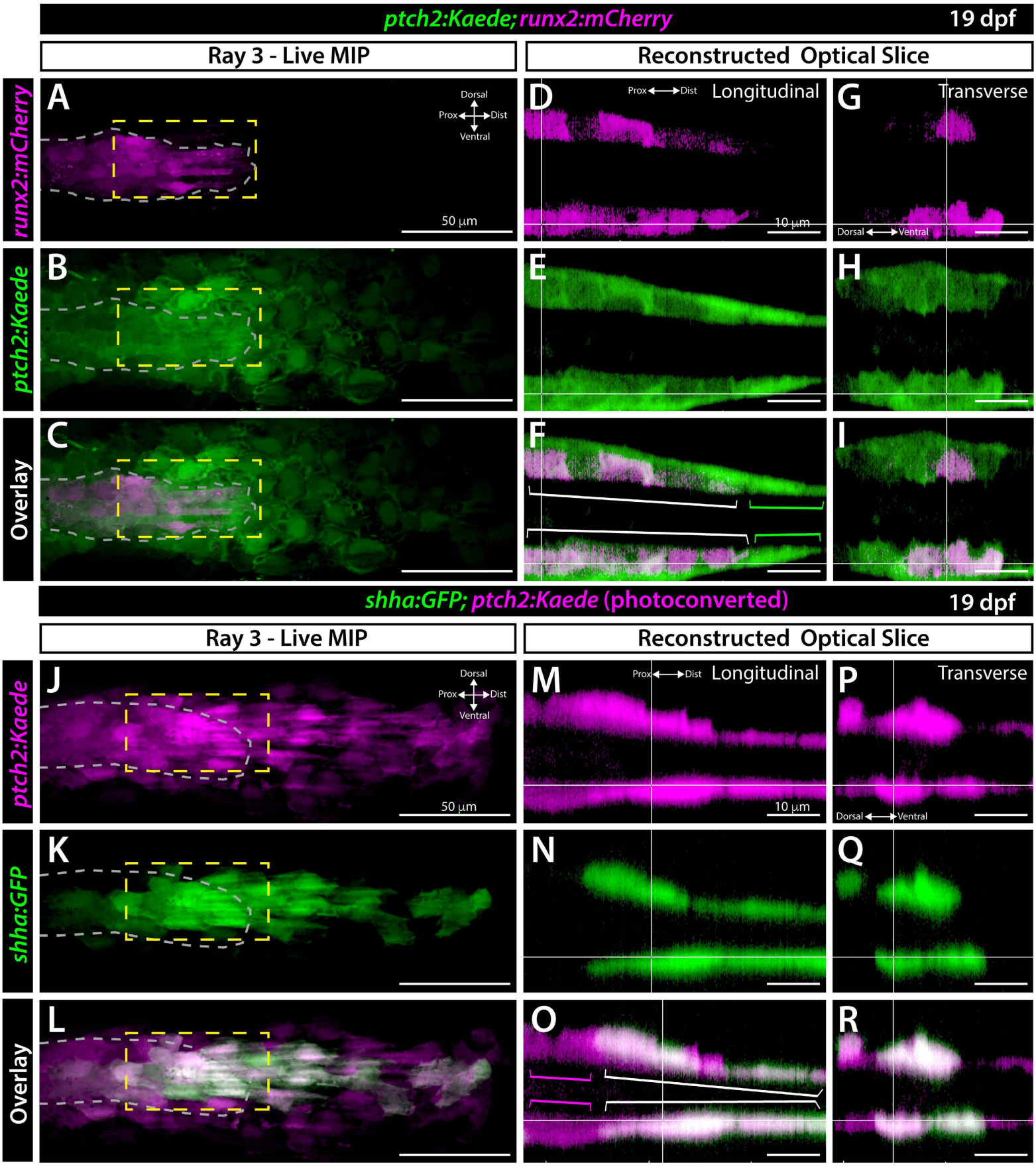

Supplemental Figure 4

Figure S4. *ptch2* is expressed in tightly associated layers of distal basal epidermal cells and pre-osteoblasts in developing caudal fins.

(A-I) Whole mount confocal imaging of dorsal ray 3 from a live 19 dpf *ptch2:Kaede; runx2:mCherry* caudal fin. (A-C) Maximum intensity projection (MIP) of a frontal view. The pre-osteoblast pool is outlined with grey dashed lines. *runx2:mCherry*-marked pre-osteoblasts are in magenta (A) and *ptch2:Kaede* is in green (B). The overlay is shown in (C). (D-I) Reconstructed optical slice views of the region marked by yellow dashed lines in A-C. Overlays (F, I; reproduced in main Figure 1) show relatively proximal regions of *ptch2:Kaede* and *runx2:mCherry*+ co-expressing pre-osteoblasts (white brackets) and an adjacent thin layer of *ptch2:Kaede*+ basal epidermal cells. These basal epidermal cells extend further distally from the pre-osteoblast pool (green brackets). (J-R) Confocal images of dorsal ray 3 from a 19 dpf *shha:GFP;ptch2:Kaede* caudal fin in which the Kaede protein has been photoconverted from green to red fluorescence emission. (J-L) Frontal view MIP with osteoblast-populated region outlined with grey dashed lines. *shha:GFP* basal epidermis (green) co-express *ptch2:Kaede* (magenta). (M-R) Reconstructed optical slices of the yellow dashed boxes in J-L. Overlays (O, R; reproduced in main Figure 1) demonstrate proximal regions contain single-positive *ptch2:Kaede*+ pre-osteoblasts (magenta brackets) whereas distal regions include co-expressing *shha:GFP* and *ptch2:Kaede* basal epidermis (white brackets). Scale bars are 50 μm in A-C, J-L and 10 μm in D-I, M-R.

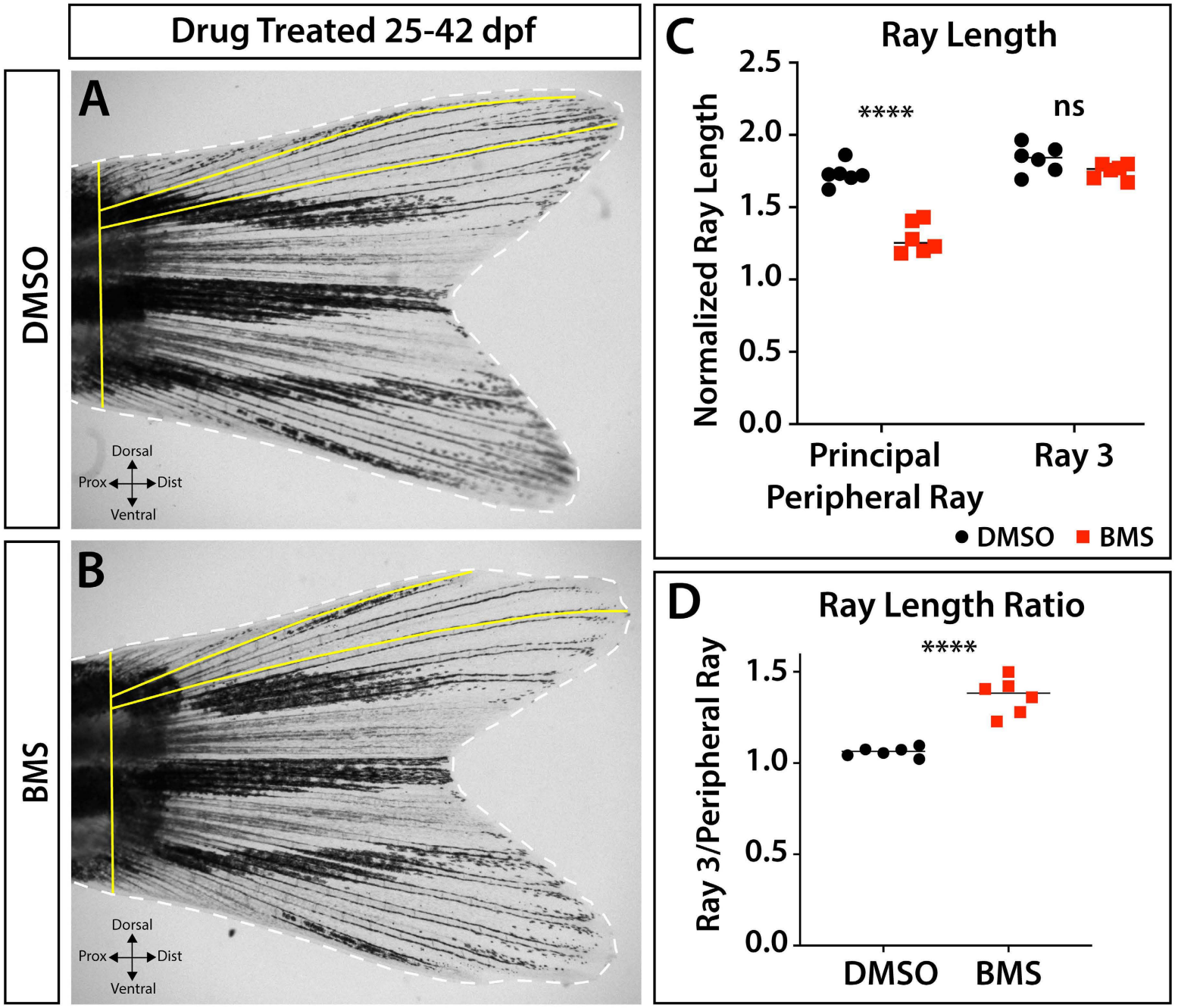

Supplemental Figure 5

Figure S5. Shh/Smo signaling contributes to principal peripheral ray outgrowth.

Whole mount caudal fin images of (A) DMSO- and (B) BMS-treated juvenile fish (exposed from 25-42 days post fertilization (dpf)) and (C) graphs of ray morphometrics. Yellow lines indicate measured ray lengths and fin widths. Dorsal ray 3 does not significantly differ in length between treatment groups ($p = 0.09$). In contrast, the non-branching principal peripheral ray 1 is uniquely shorter in BMS-treated versus DMSO control fish ($p < 0.0001$). As such, the ray length ratio between ray 3 and principal peripheral ray 1 is higher in BMS-treated fish ($p < 0.0001$). Images are representatives of experimental groups of n=6. Ray length measurements are from the base of the fin and are normalized to fin width, which did not differ between groups. Statistical significance was determined using Student's unpaired t-tests.

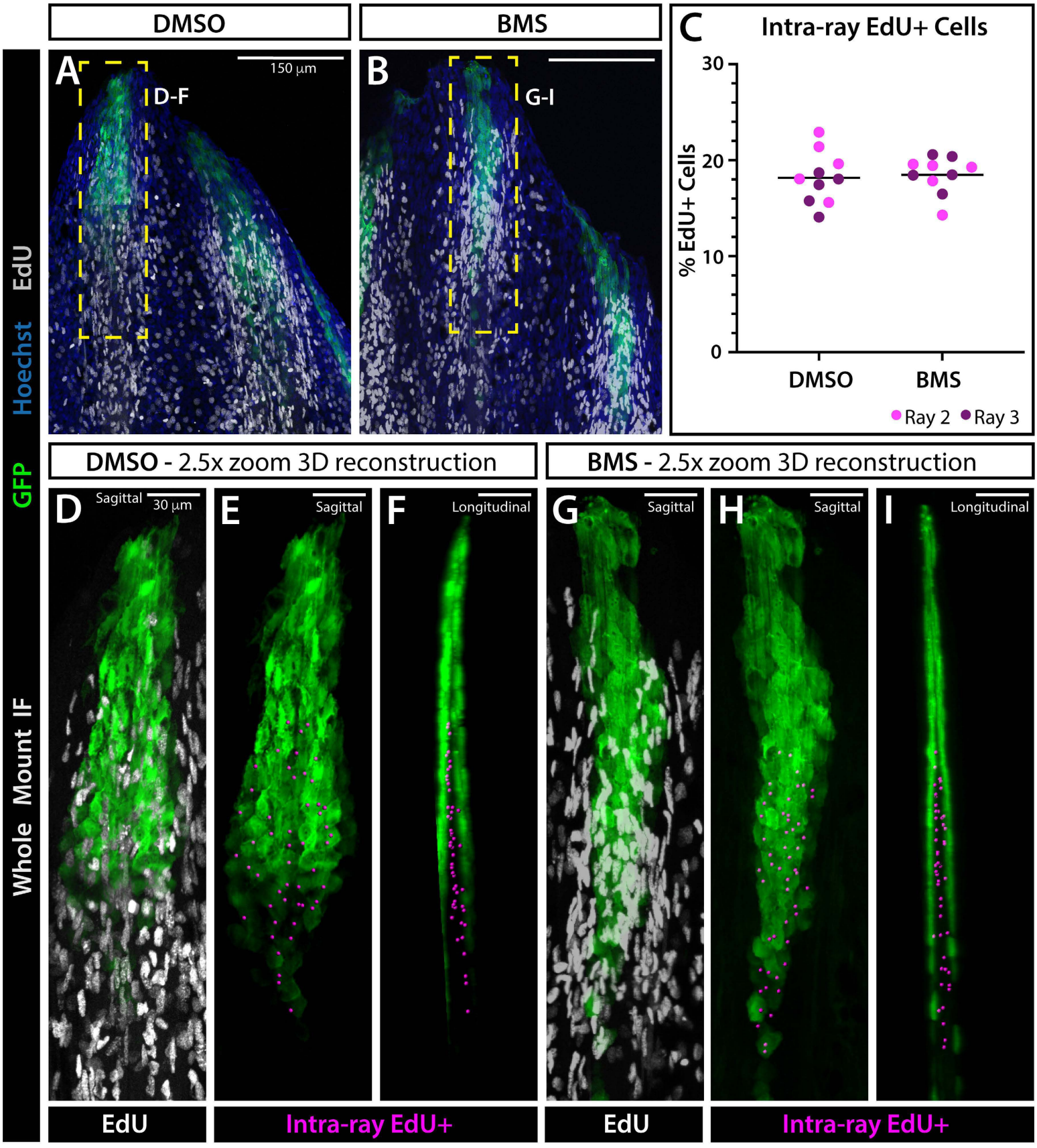

Supplemental Figure 6

Figure S6. Shh/Smo signaling does not impact proliferation in developing fin rays.

(A, B) Confocal maximum intensity projection images of whole mount immunostained 29 dpf developing *shha:GFP* caudal fins. Fish were treated with DMSO (A) or BMS-833923 (BMS) (B) for 4 hours, IP injected with EdU, returned to drug, and fins harvested 12 hours later. GFP is in green, Hoechst nuclear stain in blue, and EdU as detected with Click-iT Plus in white. (C) Dot plot graph showing the percent of intra-ray EdU+ cells, i.e. those located in between the epidermal Shh domains of each hemi-ray, does not significantly differ between DMSO controls and BMS-treated fish. n=5 for each group. (D-I) 3D reconstructions of ray 3 domains marked by yellow dashed boxes in (A, B). (D, G) Overlay of GFP and EdU, sagittal view. (E, H) GFP with magenta spheres marking EdU+ cells located within the intra-ray space, detected and quantified with Imaris software. (F, I) Longitudinal view of (E, H). Intra-ray EdU+ cells are located in between Shh+ domains with epidermal cells excluded from automated scoring. Scale bars are 150 μm or 30 μm, as indicated.

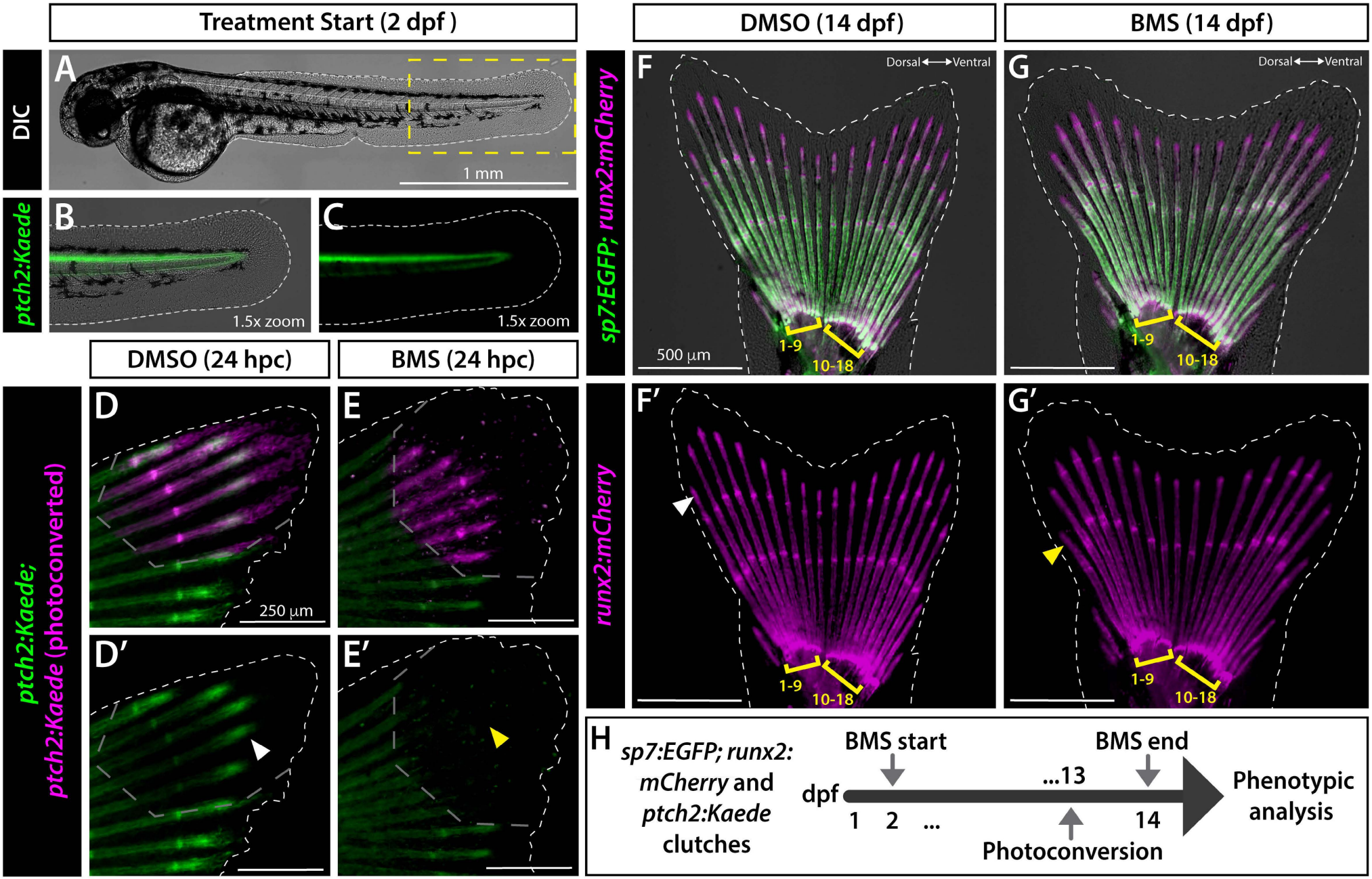

Supplemental Figure 7

Figure S7. Shh/Smo signaling does not influence initial caudal fin patterning.

(A-C) Whole mount differential interference contrast (DIC) and/or fluorescence images of a 2 dpf *ptch2:Kaede* embryo. The dashed yellow box marks the 1.5x zoomed region shown in (B, C). The primordial fin fold lacks rays or structural ray precursors. *ptch2:Kaede* expression is restricted to the notochord and does not expand into the fin fold. (D-E'). *ptch2:Kaede* larvae treated with DMSO or BMS-833923 (BMS) from 2 dpf, photoconverted distal fin regions at 13 dpf (grey dashed lines), and imaged 24 hours later (*n*=3-5 per group). BMS treatment blocked production of new green Kaede (yellow arrowhead, E') compared to controls (white arrowhead, D'). (F-G') Whole mount fluorescence images of *sp7:EGFP;runx2:mCherry* larvae treated with DMSO (F) or BMS (G) from 2-14 dpf. Both groups have caudal fins with the standard complement of 18 segmented rays, with 9 rays each on the dorsal and ventral lobes (yellow brackets). BMS-treated fins exhibit shortened principal peripheral rays (yellow arrowhead, G') compared to DMSO controls (white arrowhead, F'). *n*=33 DMSO- and *n*=44 BMS-treated larvae from 2-14 dpf. Scale bars are 1 mm, 250 μm, or 500 μm, as marked.

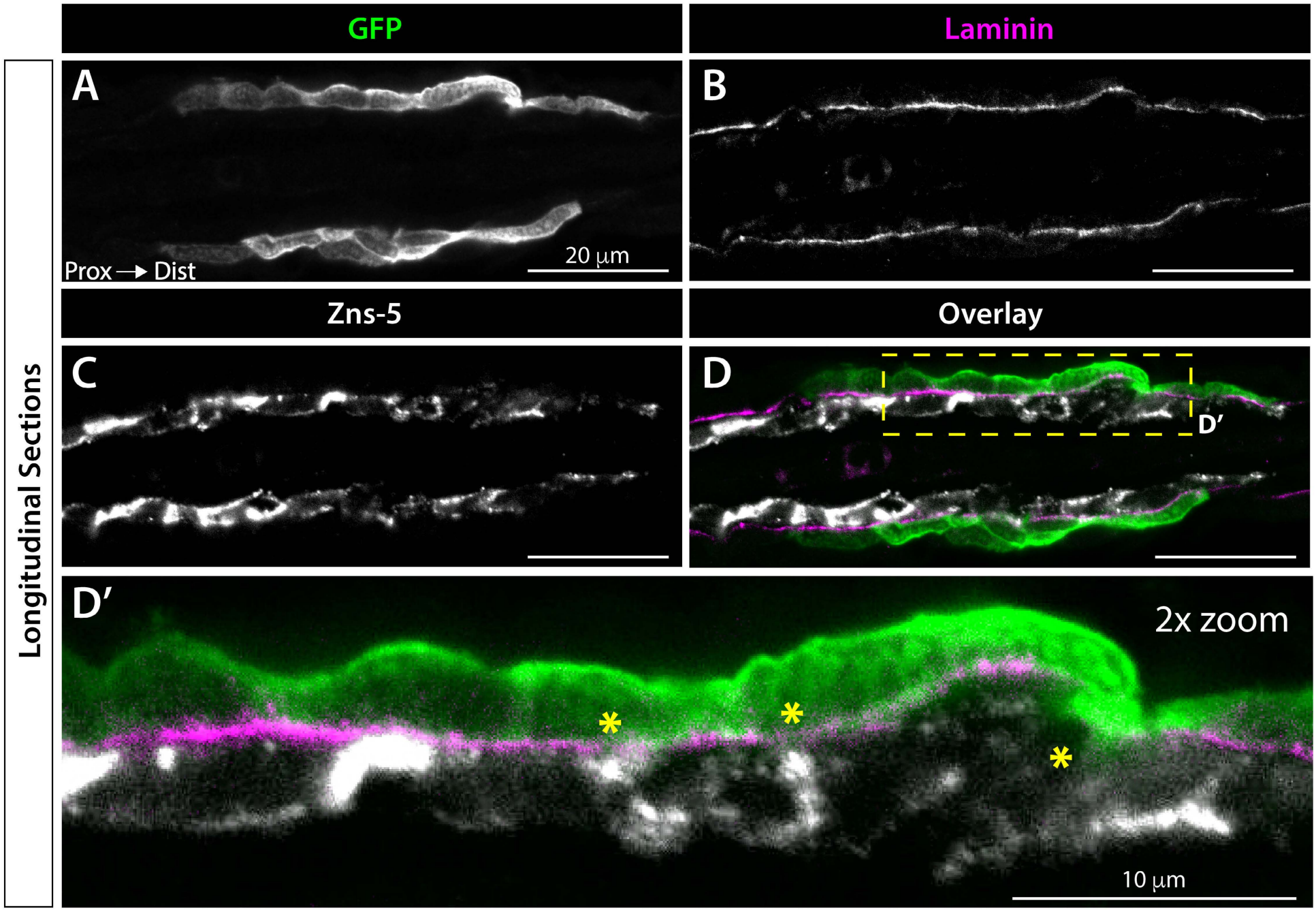

Supplemental Figure 8

Figure S8. Shha+ basal epidermal cells are tightly associated with pre-osteoblasts in distal regions of incomplete basement membrane assembly.

(A-D) Confocal images of the distal ray regions from immunostained longitudinal caudal fin sections of 32 dpf *shha:GFP* fish. GFP-expressing basal epidermal cells (green) and Zns-5-marked osteoblasts (white) are separated by a Laminin-defined basement membrane (BM; magenta). (D') 2x magnification of the yellow dashed box region in the (D) overlay. Asterisks mark areas where Laminin signal is less dense, indicating an incompletely assembled BM, and GFP and Zns-5 partially overlap (D'). Scale bars are 20 μm.

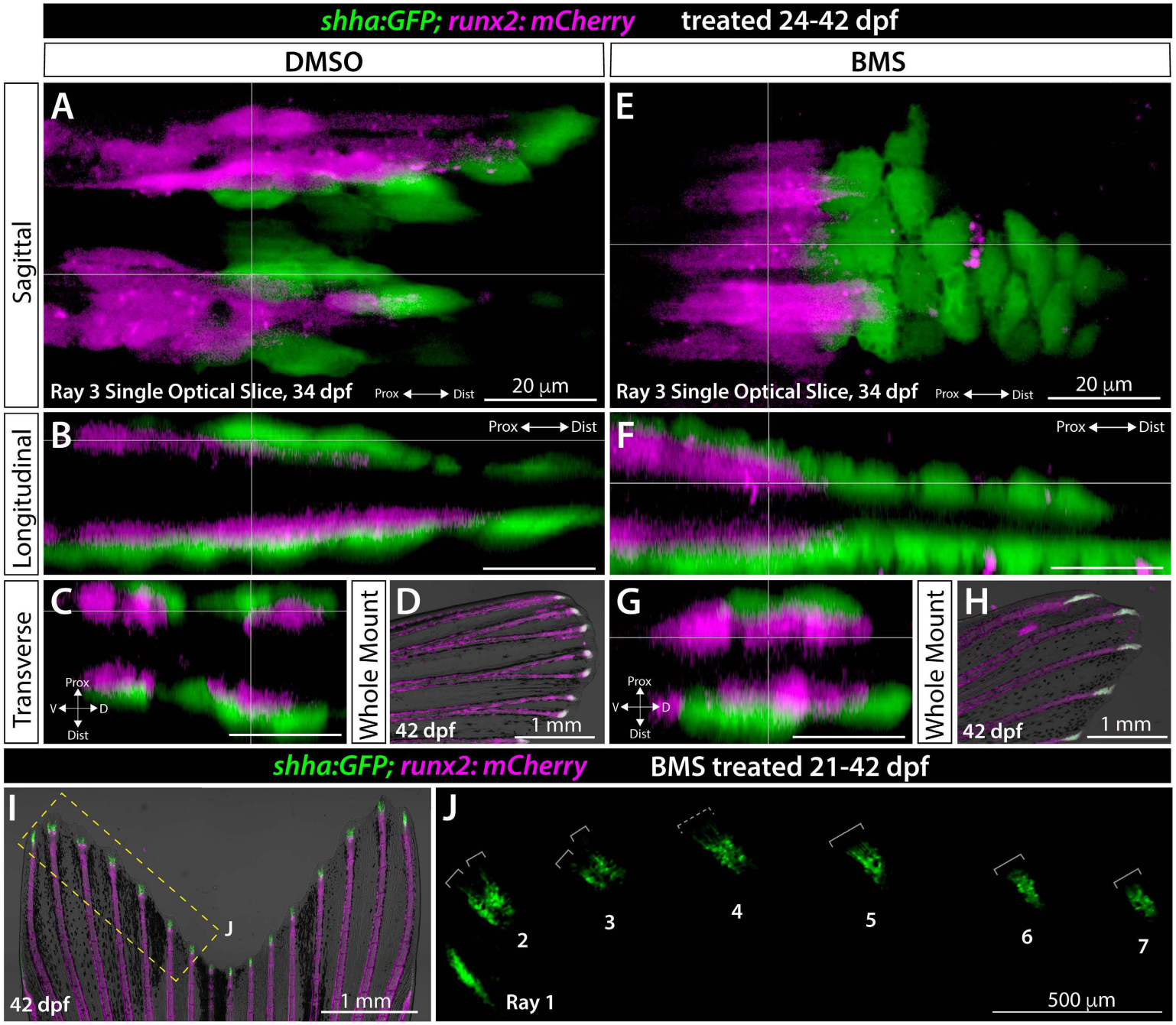

Supplemental Figure 9

Figure S9. Shh/Smo signaling does not influence Shh+ basal epidermis and pre-osteoblast juxtaposition.

(A-J) Confocal or widefield fluorescence caudal fin images from *shha:GFP;runx2:mCherry* fish treated with DMSO (control) or 1.25 μM BMS-833923 (BMS) starting at 24 dpf (*n*=8 per group). (A-C, E-G) Single optical slices or equivalent 3D-reconstructed views of 34 dpf mid-treatment fish, imaged concurrently with active ray branching morphogenesis. *shha:GFP*+ basal epidermal cells (green, A) are closely associated with *runx2:mCherry*-expressing pre-osteoblasts (magenta). BMS-treated fish (E-G) maintain close Shh+ basal epidermal and Runx2+ pre-osteoblast contacts while lacking clear *shha:GFP* domain-splitting (*n*=4 per group). (D, H, I, J) Caudal fin images of *shha:GFP;runx2:mCherry* fish continued on drug treatment until 42 dpf (*n*=4 per group). (D, H, I) Widefield fluorescence and brightfield overlay caudal fin images. Unlike DMSO controls (D), BMS-treated fish do not develop branched rays, confirming drug efficacy (H). (I, J) Fin of a 21-42 dpf BMS-treated fish. The yellow dashed box indicates the GFP-alone magnified panel in (J). *shha:GFP* domains are variably split (two grey brackets, rays 2, 3), partially split (dashed grey bracket, ray 4) or unsplit (one grey bracket, rays 5-7). Scale bars are 20 μm (A-C, E-G), 1 mm (G, H, I) and 500 μm (J).

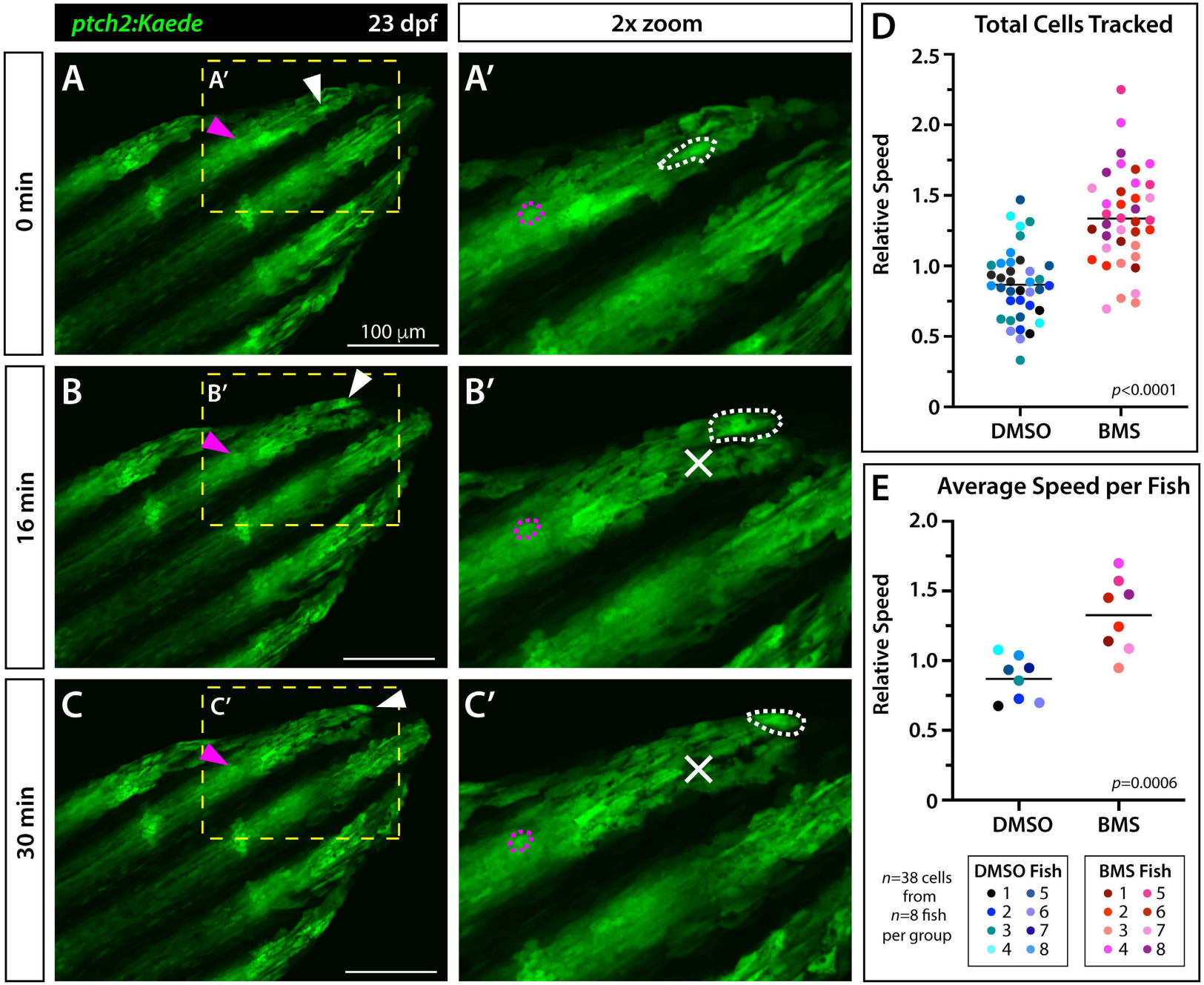

Supplemental Figure 10

Figure S10. Shh/Smo signaling restrains the distal migration of basal epidermal cells.

(A-C) Still frames from 30 minute time lapse movies capturing basal epidermal distal migration in a caudal fin of a live mounted 23 dpf *ptch2:Kaede* fish. The fish was DMSO-treated as a control group member for quantitative studies. Maximum intensity projections of a fin's dorsal lobe are shown at 0 minutes (A, start position), 16 minutes (B, halfway through video), and 30 minutes (C, end position). White and magenta arrowheads indicate a *ptch2:Kaede*+ basal epidermis and pre-osteoblast, respectively. Yellow dashed boxes mark the 3x magnified distal ray region in (A'-C'). The representative basal epidermis (white) and pre-osteoblast (magenta) are outlined with dashed lines. The white Xs in (B', C') indicate the basal epidermal cell's starting position at 0 minutes. Scale bars are 100 μm. (D) Dot plot graph showing average speeds (arbitrary units) of individual *ptch2:Kaede*+ basal epidermal cells from fish treated with DMSO or BMS-833923 (BMS) for 24 hours and then imaged over 30 minutes. Cells of BMS-treated fish migrate faster than DMSO controls ($p < 0.0001$, Student's t-test). (E) Graph showing basal epidermal migration averaged by individual animal (as indicated by different colors) is significantly faster ($p < 0.0006$, Student's t-test) in BMS-treated fish. n=3-6 cells per fish with 8 fish per treatment for a total of 38 tracked cells per group. Colors represent single basal epidermal cells from the same animal.

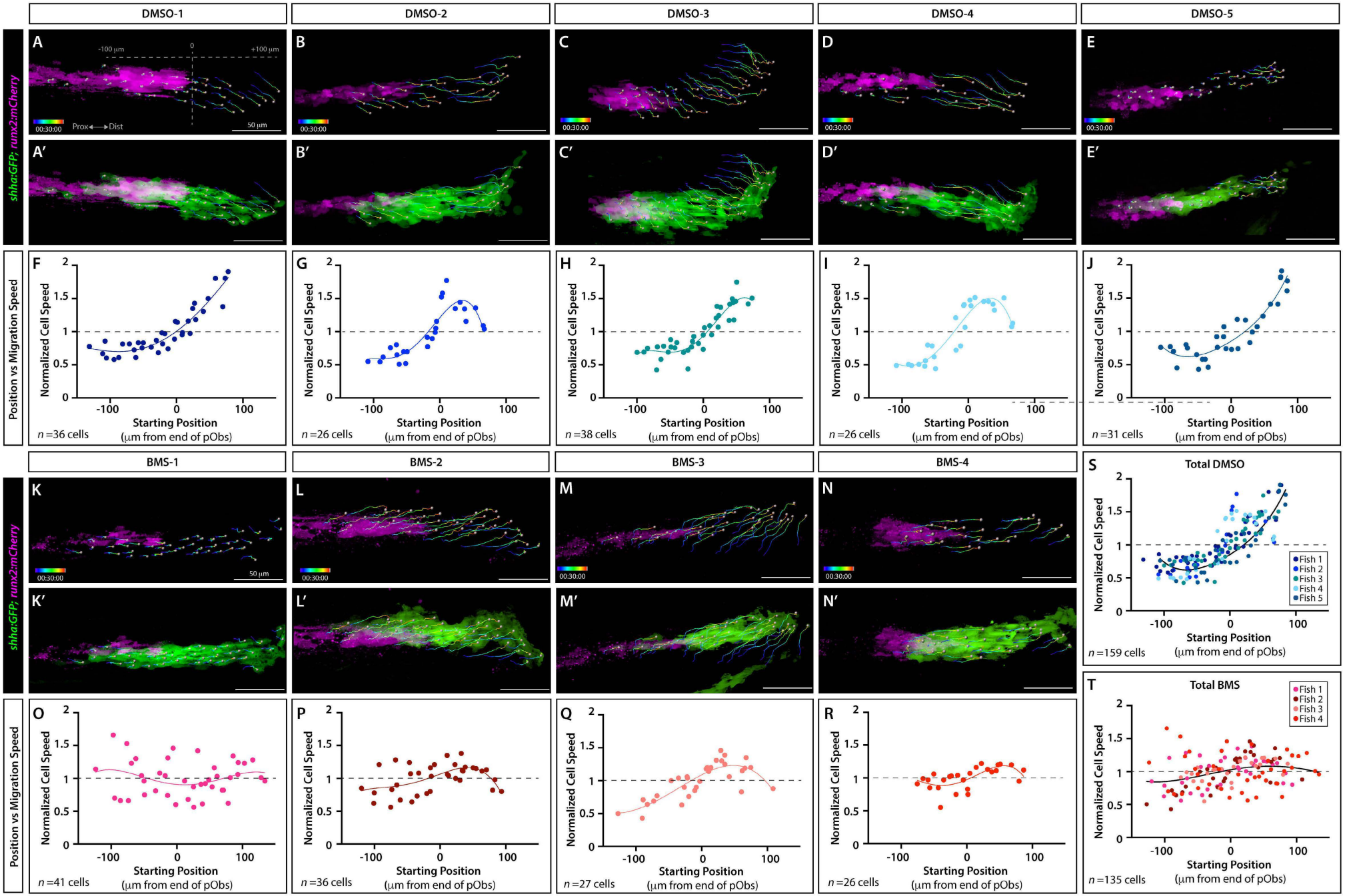

Supplemental Figure 11

Figure S11. Position- and Shh/Smo-dependent *shha:GFP*+ basal epidermal migration rates of individual fish.

Expanded data from Figure 6. (A-E', K-N') Maximum intensity projections of the final 30 minute frame of time lapse-imaged *shha:GFP;runx2:mCherry* fish (21-24 dpf) treated with DMSO (*n*=5) or BMS-833923 (BMS; *n*=4) for 24 hours. Panels show *runx2:mCherry* pre-osteoblasts only (A-E, K-N; magenta) or both pre-osteoblasts and *shha:GFP*+ basal epidermal cells (A'-E', K'-N'; green). Grey spheres mark semi-automatically tracked basal epidermal cells with their cell displacement over 30 minutes indicated by multicolor tracks. (F-J, O-T) Normalized cell speed vs. starting position scatter plot graphs for each fish. Data points represent individual cell speeds. Non-parametric best-fit curves provide a visual guide. (S, T) Summary graphs reproduced from Figure 6 show combined data with added overall trends. Scale bars are 50 μm.

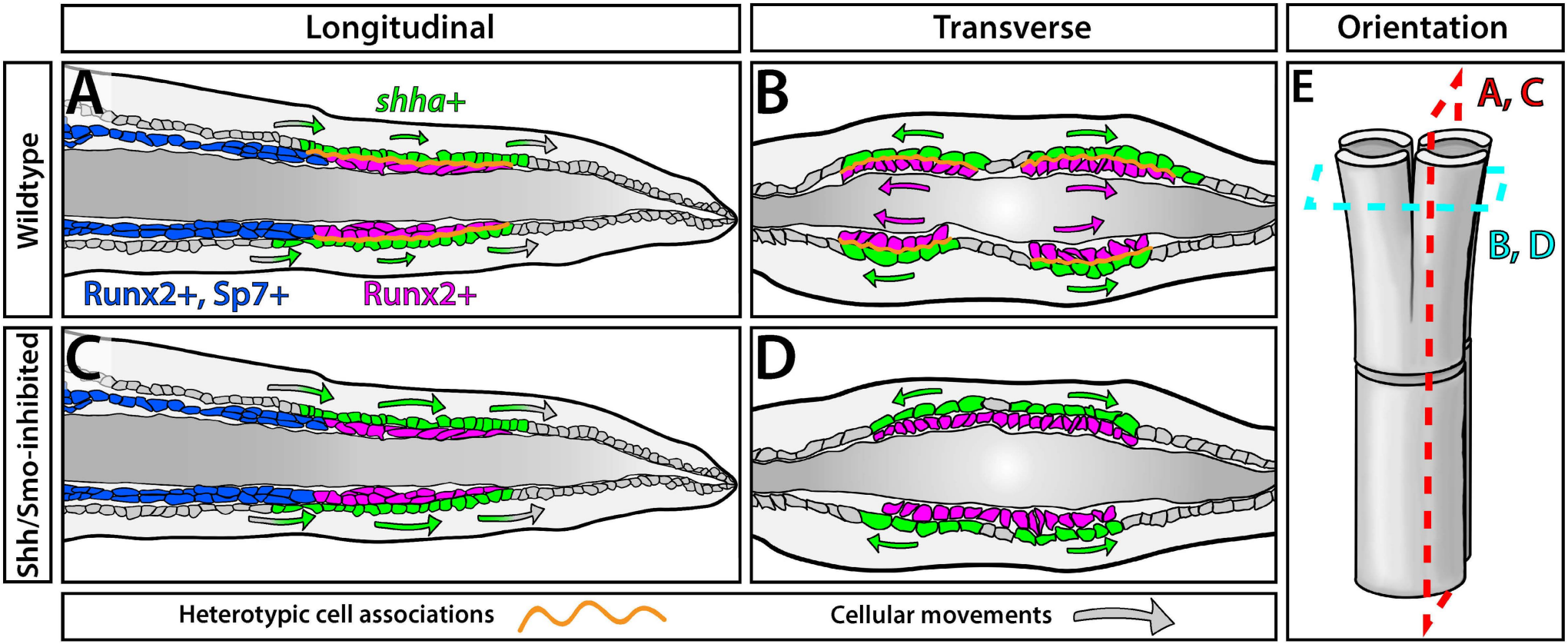

Supplemental Figure 12

Figure S12. Basal epidermis collective movements and Shh/Smo-driven heterotypic associations with pre-osteoblasts direct fin ray branching morphogenesis. (A-D) Schematics depicting the organization and cell movements of basal epidermal cells and osteoblasts during ray branching of outgrowing fins. Wildtype (A, B) and Shh/Smo-inhibited (C, D) conditions are shown. Longitudinal views (A, C) illustrate basal epidermal distal cell movements and transverse views (B, D) highlight lateral movements of both basal epidermal cells and Runx2+ pre-osteoblasts. **(E)** Schematic of a mature branched ray to orient the equivalent sectional views in (A-D). (A, C) Distal-moving basal epidermal cells (grey) enter the Shh/Smo active zone and upregulate *shha* to activate a Shh/Smo response in themselves and juxtaposed pre-osteoblasts. Shh/Smo-inhibition using the small molecule BMS-833923 increases and steadies the rate of basal epidermal distal migration (see animation in Movie 5). This suggests Shh/Smo activity normally slows the distal march of transiently Shh-expressing basal epidermal cells by enhancing cell associations (orange lines) with relatively static Runx2+ pre-osteoblasts. Basal epidermal cells downregulate *shha* and lose their Shh/Smo response as they move beyond the pre-osteoblasts. (B, D) The *shha*-expressing basal epidermal domain laterally divides, closely followed by underlying pre-osteoblast pools, prior to ray branching. BMS-833923 prevents pre-osteoblasts from following the lateral-splitting *shha*-expressing basal epidermis and thereby blocks ray branching. Shh/Smo-promoted heterotypic cell associations may transfer lateral forces from successively passaging basal epidermal cells to progressively re-position pre-osteoblasts into split pools. Each pre-osteoblast pool and their derived Runx2+/sp7+ osteoblasts now form separate daughter rays joined at a branch point.

Movie 1. A dynamic 3-D visualization of confocal-imaged caudal fin dorsal ray 3 from a 28 dpf *shha:GFP;runx2:mCherry* fish. *shha:GFP+* basal epidermis (green) of both hemi-rays are beginning to branch. Underlying pre-osteoblasts (magenta) are pressed against basal epidermis. 3D reconstruction of live confocal microscopy. Surfaces added with Imaris to visualize domain boundaries.

Movie 2. 3-D space exploration of the distal region of a confocal-imaged caudal fin hemi-ray from a 28 dpf *shha:GFP;runx2:mCherry* fish. The *shha:GFP+* basal epidermis (green) domain has started splitting ahead of ray branching. A ridge of pre-osteoblasts (magenta) is nestled in a hollow of *shha:GFP+* basal epidermis. Imaris-generated surfaces help visualize domain boundaries. Single optical slices of the same region are shown in Figure 5.

Movie 3. Time lapse movie of the dorsal lobe of the caudal fin of a live-mounted 23 dpf *ptch2:Kaede* fish treated with DMSO (control group) for 24 hours prior to imaging. Widefield fluorescence images were collected every 2 minutes over a 30-minute period. Still images and data analysis are in Figure S11.

Movie 4. Time lapse movie of caudal fin dorsal lobes of representative live-mounted *shha:GFP;runx2:mCherry* fish treated with DMSO (upper panel) or BMS-833923 (lower panel) for 24 hours prior to imaging. Shh+ basal epidermis in green and Runx2+ pre-osteoblasts in magenta were imaged by fluorescence confocal microscopy. Multicolor lines indicate cell migration tracks for individual Shh+ basal epidermal cells (marked by grey spheres) over time.

Images were acquired every 2 minutes for 30 minutes. Still images and data analysis are in Figure 6.

Movie 5. Heterotypic cell associations decrease the rate of basal epidermal distal movements while adjacent to pre-osteoblasts. This animation related to Figure S13 highlights the distal transit of single basal epidermal cells (red) in longitudinal section views of outgrowing caudal fins. (A) Basal epidermal cells constantly and collectively move distally as an interconnected epithelium, upregulating *shha* to sustain a distal Shh/Smo active zone including tightly associated pre-osteoblasts. Normally, Shh/Smo-promoted associations between basal epidermal cells and pre-osteoblasts transiently restrain the passage of basal epidermal cells. Basal epidermal cells then accelerate once passing beyond the pre-osteoblasts and losing Shh/Smo-dependent heterotypic associations. (B) Shh/Smo inhibition using BMS-833923 likely tempers associations between bEps and pObs, increasing and producing a now constant rate of basal epidermis distal migration. Basal epidermal lateral movements preceding ray branching and Shh/Smo-dependent tight associations may confer the physical force that progressively splits underlying pOb pools for ray branching morphogenesis.